Stem Cell Reports
Report
OPEN ACCESS

The Developmental Stage of Adult Human Stem Cell-Derived Retinal Pigment Epithelium Cells Influences Transplant Efficacy for Vision Rescue

Richard J. Davis,[1,7] Nazia M. Alam,[3,6,7] Cuiping Zhao,[1,7] Claudia Müller,[4] Janmeet S. Saini,[1] Timothy A. Blenkinsop,[2] Francesca Mazzoni,[4] Melissa Campbell,[1] Susan M. Borden,[1] Carol J. Charniga,[1] Patty L. Lederman,[1] Vanessa Aguilar,[1] Michael Naimark,[1] Michael Fiske,[5] Nathan Boles,[1] Sally Temple,[1] Silvia C. Finnemann,[4] Glen T. Prusky,[3,6,8] and Jeffrey H. Stern[1,8,*]

[1]Neural Stem Cell Institute, Regenerative Research Foundation, One Discovery Drive, Rensselaer, NY 12144, USA
[2]Cell, Developmental & Regenerative Biology, Icahn School of Medicine at Mount Sinai, New York, NY 10029, USA
[3]Department of Physiology and Biophysics, Weill Cornell Medical College, New York, NY 10605, USA
[4]Department of Biological Sciences, Center for Cancer, Genetic Diseases and Gene Regulation, Fordham University, Bronx, NY 10458, USA
[5]Upstate Stem Cell cGMP Facility, University of Rochester Medical Center, Rochester, NY 14642, USA
[6]Center for Visual Restoration, Burke Medical Research Institute, 785 Mamaroneck Avenue, White Plains, NY 10605, USA
[7]Co-first author
[8]Co-senior author
*Correspondence: jeffreystern@neuralsci.org
http://dx.doi.org/10.1016/j.stemcr.2017.05.016

SUMMARY

Age-related macular degeneration (AMD) is a common cause of central visual loss in the elderly. Retinal pigment epithelial (RPE) cell loss occurs early in the course of AMD and RPE cell transplantation holds promise to slow disease progression. We report that subretinal transplantation of RPE stem cell (RPESC)-derived RPE cells (RPESC-RPE) preserved vision in a rat model of RPE cell dysfunction. Importantly, the stage of differentiation that RPESC-RPE acquired prior to transplantation influenced the efficacy of vision rescue. Whereas cells at all stages of differentiation tested rescued photoreceptor layer morphology, an intermediate stage of RPESC-RPE differentiation obtained after 4 weeks of culture was more consistent at vision rescue than progeny that were differentiated for 2 weeks or 8 weeks of culture. Our results indicate that the developmental stage of RPESC-RPE significantly influences the efficacy of RPE cell replacement, which affects the therapeutic application of these cells for AMD.

INTRODUCTION

Age-related macular degeneration (AMD) is a leading cause of blindness in the developed world (Wong et al., 2014). There are two major subtypes of AMD: non-exudative or dry AMD, which is characterized by subretinal accumulation of extracellular lipid-protein deposits termed drusen accompanied by RPE cell atrophy, and later stage exudative or wet AMD that occurs after ingrowth of the underlying choroidal vasculature into the retina (Gass, 1997). Dry AMD constitutes about 90% of AMD cases in the US, and there is currently no effective disease-altering therapy for this highly prevalent disorder.

RPE cells provide essential support to the retina by regulating ionic and fluid balance, providing cytokines, forming the blood-retina barrier, regenerating photoreceptor visual pigment and phagocytosing and recycling photoreceptor outer segments. As RPE cells atrophy in AMD, support of overlying photoreceptors declines, leading to vision loss. This occurs predominantly in the macula (central region of retina), which is responsible for color and high acuity vision. Impaired central vision that occurs due to AMD is debilitating, with loss of the ability to read, recognize faces, and a concomitant loss of independence.

Surgical transplantation (Algvere et al., 1997) or translocation (van Meurs and Van Den Biesen, 2003) of RPE sheets into the macula preserves central vision, providing proof of concept that RPE transplantation can be beneficial in AMD (reviewed in Binder et al., 2007). Stem cell technology now provides ample sources of RPE cells for transplantation to counteract RPE cell loss in AMD. Pluripotent stem cells (PSCs), embryonic stem cells (ESCs), and induced pluripotent stem cells have been successfully differentiated into RPE (Buchholz et al., 2009; Klimanskaya et al., 2004), and early stage clinical trials transplanting ESC-derived RPE suspensions report safety and preliminary benefit (Schwartz et al., 2012, 2015; Song et al., 2015). An important concern with PSC-derived RPE is the possibility of overgrowth and mis-differentiation due to residual undifferentiated source cells; this has been addressed by extensive differentiation into the RPE phenotype prior to transplantation (Kanemura et al., 2014). The influence of RPE differentiation stage on transplant efficacy, however, has not been described. We used an adult RPE stem cell, which is less plastic than PSC and does not form tumors, to determine the influence of RPE differentiation stage on transplant outcome.

The human RPE layer contains a minor subpopulation of cells that by stringent clonal analyses and other tests fulfill the criteria of stem cells, namely they can self-renew and produce differentiated progeny; these are adult RPE stem cells (RPESCs) (Salero et al., 2012). RPESCs are poised to

This is an open access article under the CC BY-NC-ND license (http://creativecommons.org/licenses/by-nc-nd/4.0/).

generate highly pure cultures of RPE progeny (RPESC-RPE) displaying characteristics of native RPE (Blenkinsop et al., 2015). We previously reported that subretinal transplantation of RPESC-RPE in the Royal College of Surgeons (RCS) rat prevents the loss of photoreceptor cells that occurs in these animals (Davis et al., 2016). Here, we report that transplantation of RPESC-RPE effectively rescued vision (i.e., prevented vision loss that normally occurs in the RCS rat) in a differentiation stage-dependent manner. Specifically, transplantation of an intermediate 4-week stage of RPE differentiation most consistently preserved vision.

RESULTS

RPESC Differentiate and Mature with Prolonged Culture

RPESCs were obtained from donor eyes using methods described previously (Blenkinsop et al., 2013, 2015; Salero et al., 2012) and frozen at passage 1 (P1) (Figure 1A, schematic). P1 cells were plated at 1×10^5 cells per well in Synthemax-coated 24-well plates and cultured in RPE medium. All experiments were performed on resulting passage 2 (P2) cultures. Three RPESC lines derived from three independent donors were utilized.

Phase microscopy of live P2 cultures showed that most cells were initially fusiform (Figure 1B). With continued culture, clusters of cuboidal cells emerged at around 4 weeks, and by 8 weeks of culture the majority of the cells acquired a mature, cobblestone RPE morphology. During the RPE differentiation process, the number of proliferating cells declined, indicated by decreased expression of the proliferation marker Ki67 (Figures 1C and S1) from about 5% of cells at 2 weeks to minimal levels after 6 weeks. Vascular endothelial growth factor A (VEGF-A) secretion across the apical and basal membranes increased from 2 weeks to 4 weeks, while polarized pigment epithelium-derived factor (PEDF) secretion not present at 4 weeks emerged by 6 weeks (Figure 1D). Transepithelial resistance is known to increase over this time period (Blenkinsop et al., 2015; Stanzel et al., 2014). In addition, RPESC-RPE showed increased localization of ZO-1 to the lateral cell borders (Figure 1B). Over the 8-week differentiation period, RPESC-RPE continuously expressed the RPE cell fate determination factors OTX2 and MITF (Figure 1B) and did not express smooth muscle actin (Figure S1), an indicator of epithelial-to-mesenchymal transition. Under these growth conditions, RPESC-RPE cultures from three different donors consistently progressed through specific stages of maturation to acquire the RPE phenotype over a period of about 8 weeks.

Daily phagocytosis of photoreceptor outer segment fragments (POS) by the RPE is essential for long-term photoreceptor maintenance. We tested the ability of RPESC-RPE cells at different stages of differentiation to phagocytose POS using a standardized POS uptake assay (Figure 2A) (Mao and Finnemann, 2013). Confocal immunofluorescence image analysis was used to quantify bound and internalized POS in fixed RPESC-RPE monolayers (see Supplemental Experimental Procedures and Figure S2). We found, in three independent RPESC lines, that 60%–70% of RPESC-RPE cells internalized POS within 5 hr after 2–3 or 4–5 weeks in culture (Figures 2B and 2C). In contrast, the fraction of actively phagocytic RPESC-RPE after 7 weeks in culture decreased significantly to ~39% (Figures 2D, 2E, and 2F). The amount of POS material that RPESC-RPE cells engulfed also declined significantly over the 4- to 7-week culture period (Figures 2E and 2F). Immunoblotting conducted on RPESC-RPE at different stages showed no decline with time in levels of the phagocytic receptor MERTK or the subunits of the POS-binding receptor αv and β5 integrins (Figure S3).

RPESC-RPE at All Stages Rescue ONL Morphology

The RCS rat is a commonly used model to develop cell therapy for AMD and has been validated by enabling clinical studies of AMD. Due to MERTK deficiency, and associated inability to phagocytose POSs, the RCS rat retina gradually loses photoreceptor cells in the outer nuclear layer (ONL), which declines from a normal depth of about eight cells to a single layer by the second month of life (LaVail, 2001). Suspensions of 50,000 passage 2 RPESC-RPE at 2, 4, or 7–8 weeks of differentiation were transplanted into postnatal day 30 (P30) rats (Figure 3A), with histological analyses at P100. The distinct lamination of normal rat retina, consisting of photoreceptor ONL, inner nuclear layer (INL), and ganglion cell layer (GCL) (Figures 3A) was lost in untreated RCS rats over the P30 to P100 time period, with only a few residual photoreceptor nuclei visible adjacent to the INL (white arrows in Figure 3A) (Bourne and Gruneberg, 1939; LaVail, 2001; LaVail et al., 1975). In contrast, injected eyes showed extensive ONL preservation in a zone adjacent to the injection site (Figures 3A and 3B) after transplantation of RPESC-RPE that had been differentiated for 2, 4, or 7–8 weeks. ONL preservation did not occur in untreated animals or those injected with control vehicle BSS (balanced salt solution).

To quantify anatomic preservation, ONL photoreceptor nuclei were counted across the retina, with spatial distribution plotted as the ONL number along both superior-inferior and nasal-temporal axes (Davis et al., 2016). Transplants survived, and most cells engrafted were found aligned along the rat RPE layer, with occasional clumps of cells also observed (Figure S4). Photoreceptor

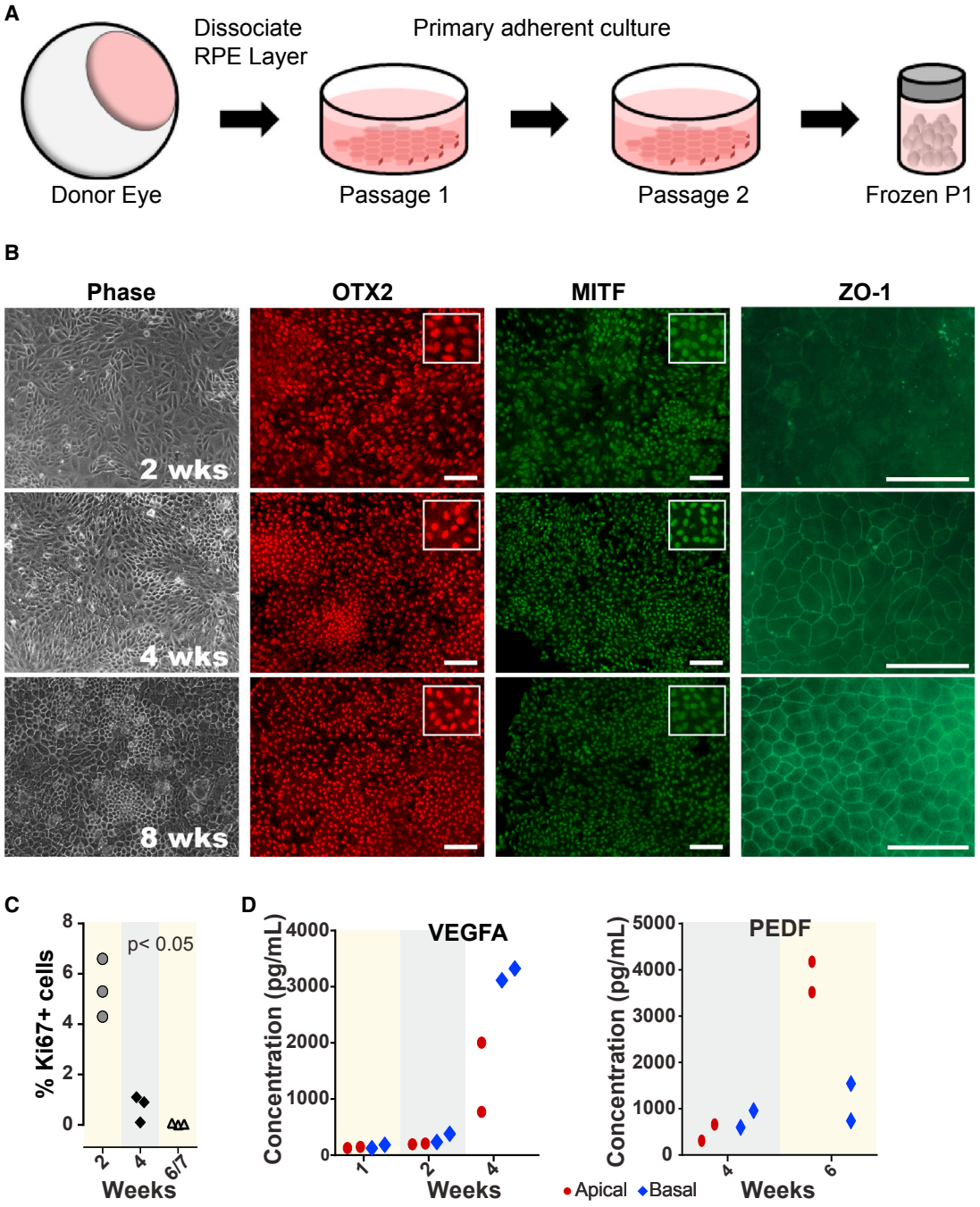

Figure 1. RPESC-RPE Mature over 8 Weeks in Culture

(A) Passage 0 (P0) RPE cells dissociated from donor cadaver eyes were expanded in culture, re-plated, re-expanded, and then frozen at passage 1 (P1).

(B) Banked P1 cells were thawed and cultured to obtain passage 2 (P2) cells at 2-, 4-, or 8-week stages. Representative phase and immunostained images are shown for OTX2, MITF, or ZO-1 expression. Insets show digitally zoomed high magnification images. Scale bar, 50 μm.

(C) The fraction of cells expressing Ki67 (Ki67+/DAPI) at 2, 4, and 6/7 weeks. One-way ANOVA ($p < 0.01$) followed by Tukey's multiple comparison test (2 versus 4, $p = 0.0006$; 2 versus 6/7, $p = 0.0003$; 4 versus 6/7, not significant).

(D) Secretion of VEGF-A (left) and PEDF (right) from apical and basal surfaces on a transwell membrane also rise during the 8-week RPE maturation period.

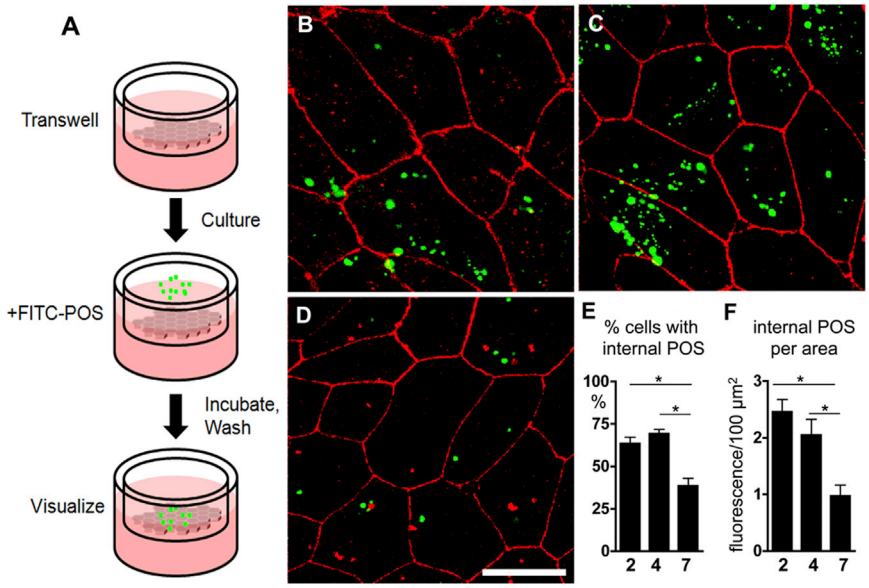

Figure 2. Phagocytic Activity of RPESC-RPE with Maturation

(A–D) RPESC-RPE cultured on transwell membrane (A) for 2–3 (B), 4–5 (C), or 7–8 weeks (D) were challenged with FITC-labeled POS (B–D). Representative confocal central image stacks show the distribution of internalized POS in green. ZO-1 labeling (red) indicates tight junctions.

(E and F) Quantification shows the percentage of cells with internalized POS (E) and the amount of internalized POS per area (F) after 5 hr of POS exposure, expressed as mean ± SEM from three different cell lines for each stage of maturation (shown in weeks, x axes). Asterisks indicate significant differences between groups indicated by horizontal bars; * = $p < 0.05$ by ANOVA. Scale bar, 20 µm.

cell preservation extended beyond the temporal injection site with an average temporal ONL thickness of 2–4 nuclei, as illustrated for 4-week cells in Figure 3B. The extent of morphologic rescue was comparable for each 2-, 4-, and 7-week stage of RPESC-RPE differentiation tested (Figure 3C) using three independent RPESC-RPE lines assessed in 17 animals.

An Intermediate 4-Week RPESC-RPE Stage Is More Efficient at Preserving RCS Rat Visual Behavior

While anatomic preservation was similar for the stages of differentiation tested, this was not the case for vision rescue. Three lines of RPESC-RPE differentiated for 2, 4, or 7–8 weeks were injected into 55 animals subretinally at approximately day P30 (Figure 4). Vision assessments were performed at 3 months (P90) of age by assessing spatial frequency thresholds (Figure 4A) using optokinetic tracking (OKT) (McGill et al., 2004; Prusky et al., 2004). To measure vision using OKT, animals are placed on a central platform surrounded by computer-generated rotating dark stripes that they follow reflexively. Stripe thickness is gradually reduced until the visual stimulus is no longer detected and this threshold for tracking head motion is recorded as visual acuity.

Without intervention, visual function was near normal at P30 and subsequently declined to 27% of normal by P90 (Figures 4B and 4C), consistent with prior reports (McGill et al., 2004, 2007). The decline in visual function of control vehicle-only (BSS) injected rats mirrored that of un-operated controls (Figures 4B and 4C). In contrast, RPESC-RPE transplantation preserved visual function (Figures 4B, 4C, and 4D). Importantly, the benefit of transplantation was significantly greater for RPESC-RPE cells that had been differentiated for 4 weeks compared with 2 weeks or 7–8 weeks. Figure 4B shows that vision was maintained near normal after transplantation of 4-week RPESC-RPE, with significantly less benefit from 2-week cells, which were not significantly different from BSS. Transplantation of 3-week or 8-week cells showed significant improvement compared with 2 weeks but this was less than the improvement seen with 4-week cells (Figure 4B). Comparison with two additional RPESC-RPE lines showed complete vision rescue after transplantation of 4-week RPESC-RPE and less consistent rescue using 7-week cells (Figure 4C). Combined data from each line in Figures 4B and 4C showed that rescue by 7- to 8-week lines was significantly less than that of 4-week lines (Figure 4D). Hence, while the stage of the RPESC-RPE over the range tested did not influence anatomic photoreceptor rescue, the stage of differentiation had a significant role in visual rescue.

DISCUSSION

Stem cell-derived RPE cells are being advanced into the clinic as a cell replacement therapy for AMD and related blinding disorders. We report that the stage of RPE differentiation influences the ability of transplanted RPE to rescue vision. Correlation of transplant efficacy with an intermediate stage of development has been reported for other cell types, such as photoreceptor cells (MacLaren et al., 2006), glia (Warrington et al., 1993), and dopaminergic neurons (Brundin et al., 1986; Ganat et al., 2012). Consistent with the prior findings using other cell types, our results indicate that transplanting an intermediate

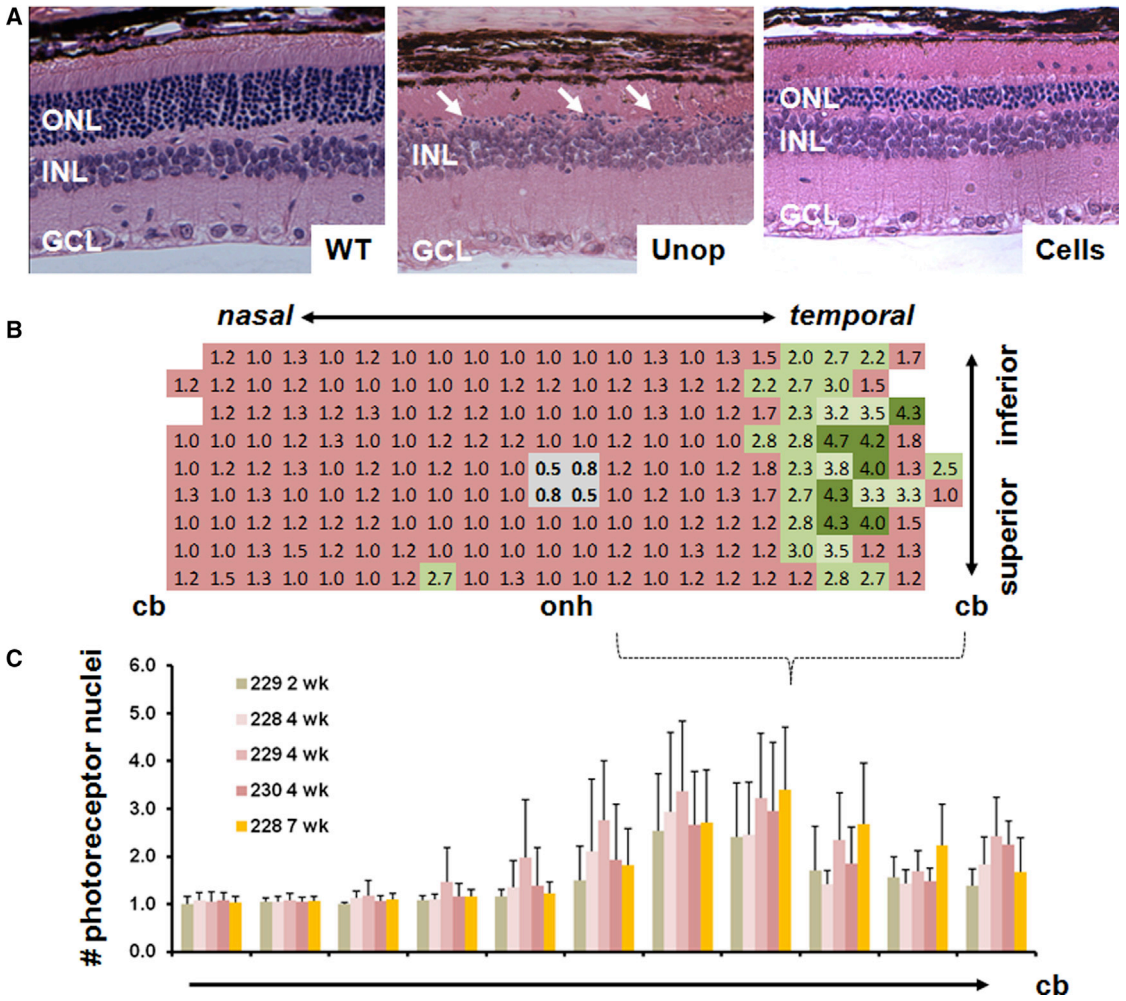

Figure 3. RPESC-RPE Transplantation Photoreceptor Rescue

(A) H&E stained retinal sections from wild-type Long Evans (WT), and P100 unoperated (Unop) or RPESC-RPE transplanted (Cells) RCS rat retinas. White arrows indicate loss of ONL.

(B and C) Quantification of ONL rescue after RPESC-RPE transplantation into the temporal region of the eye. (B) Matrix and (C) graphical representations of DAPI-stained nuclei counts across the nasal-temporal and inferior-superior axes. Rows contain the average number of nuclei over ~100–150 μm intervals. Columns contain counts from slides spaced at 200 μm intervals. cb, ciliary body; onh, optic nerve head. (B) Average counts from an RPESC-RPE injected eye. (C) Comparison of the number of rescued photoreceptor nuclei in 17 rats after subretinal injection with 2, 4, or 7 week RPESC-RPE in the temporal region (bracket in B). Three donor lines were used as follows: 228, 4 weeks, 2; 228, 7 weeks, 3; 229, 2 weeks, 3; 229, 4 weeks, 5; 230, 4 weeks, 4. Error bars indicate SD; no significant difference was observed between the 2-, 4-, and 7-week developmental stages tested.

progenitor stage of RPE differentiation improves transplant efficacy for vision rescue.

RPESC derived from human donor eyes differentiate into mature RPE over a period of several weeks in culture. During this time, cells undergo continuous changes in morphology, proliferation rate, polarization, and acquisition of key RPE phenotypic characteristics (Blenkinsop et al., 2013, 2015; Salero et al., 2012; Stanzel et al., 2014). The features of maturing RPE cells responsible for the improved ability to rescue vision at 4 weeks remain to be uncovered. However, here we report the finding that the phagocytic activity of RPESC-RPE declines after 4 weeks of maturation, which is also the time of maximum efficacy at vision rescue. This correlation raises the possibility that phagocytic activity may contribute to the stage dependence of vision rescue. Phagocytic ability was not significantly different between the 2- and 4-week stages, however, indicating that this alone could not explain the differences in efficacy at vision rescue. Although much remains to be learned about the mechanisms that confer improved

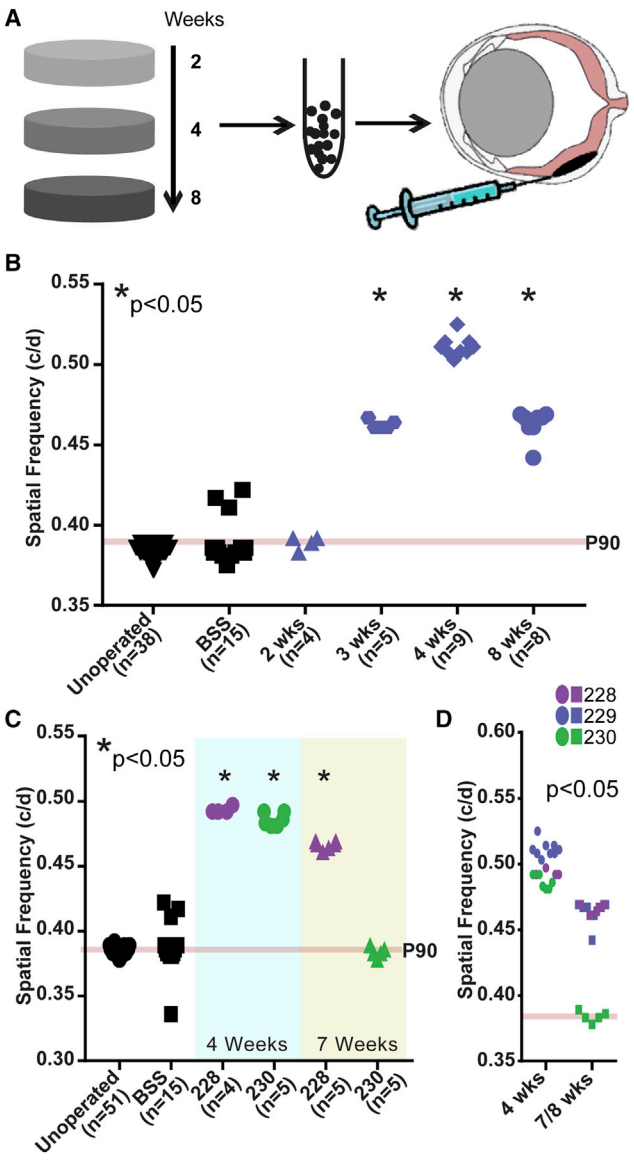

Figure 4. Stage-Dependent RPESC-RPE Transplantation Vision Rescue

(A) RPESC-RPE cultured for 2, 4, or 7–8 weeks were transplanted into 55 RCS rats.

(B) Spatial frequency thresholds were measured (cycles/degree) at P90 after transplant of 50,000 line 229 RPESC-RPE grown for 2–8 weeks. Cells differentiated for 3, 4, or 8 weeks rescued vision more effectively than 2-week cells or unoperated and BSS injected controls (* = $p < 0.05$ compared with BSS control). Other significant differences are: unoperated versus 3, 4, and 8 weeks, $p < 0.01$; and 2 versus 4 weeks, $p < 0.05$.

(C) Line 228 and 230 data at 4 and 7 weeks compiled from five experiments. * = $p < 0.05$ indicates comparison with BSS controls. Other significant comparisons are: unoperated versus 228 at 4 and 7 weeks and 230 at 4 weeks, $p < 0.01$; 228 at 4 and 7 weeks versus 230 at 8 weeks, $p < 0.01$; and 230 at 4 weeks versus 230 at 7 weeks, $p < 0.01$. Statistical analysis was a Kruskal-Wallis test ($p < 0.0001$) followed by Dunn's multiple comparisons test and correction by the two-stage Benjamini, Hochberg, Yekutieli false discovery rate method.

(D) To compare 4 week cells with 7/8 week cells, data from (B) and (C) were grouped and analyzed using a Mann-Whitney test, which indicated that 4-week cells rescued vision more effectively than 7- to 8-week cells ($p < 0.0001$).

efficacy to less differentiated cells, improved migration, integration, and continued differentiation after transplantation are thought to influence the ability of transplanted stem cell progeny to replace host tissue (Conboy et al., 2015). The possibility that intermediate RPE progenitor states engraft and survive better than mature cells has potential impact on decisions whether to implant RPE as a scaffold (Diniz et al., 2013) or as a suspension (Schwartz et al., 2012), because if a particular stage of RPE cells integrates well, they may not need to be delivered on a scaffold in order to replace the host RPE monolayer. Future studies will be aimed at identifying the mechanisms that confer transplant efficacy to specific stages of RPESC development.

We found that the developmental stage of transplanted RPESC-RPE influenced preservation of vision but not preservation of photoreceptor cells. Although the underlying explanation for this divergence is unknown, one possibility is that the developmental stage influences cones more than rods. RCS rat retinas are composed predominantly of rods, which determine ONL morphology, and rods respond to dim, scotopic light stimuli. In contrast, the smaller population of cones present in the RCS rat contribute few nuclei to the ONL and respond to the bright, photopic light stimuli (Alam et al., 2014) used in our experiments. Since our measurements of ONL morphology selectively reflect rod survival and our measurements of OKT visual acuity selectively reflect cone visual function, it is reasonable to speculate that the observed stage dependence of vision preservation arose from cone rescue. The possibility that there are different factors responsible for rod and cone rescue is important to consider when developing a cell therapy for diseases in which cones are preferentially lost, such as AMD.

In summary, the stage of adult RPESC differentiation influences the efficacy of RPE replacement therapy. In this regard, RPE cells are similar to diverse lineages, and it will be fascinating to uncover whether there are commonalities in the underlying mechanisms that improve the ability of transplanted cells to integrate and acquire functional properties in situ. Our studies address the risk-benefit balance associated with transplanting highly mature RPE cells that, while being more stable, may also have reduced efficacy, versus the use of younger, more reparative cells.

EXPERIMENTAL PROCEDURES

Human RPESC-RPE

Adult RPE cells were derived from cadaveric globes donated to registered eye banks. The retina was removed and the RPE layer was dissociated by enzymatic treatment followed by gentle trituration. Isolated adult human RPE were then activated to proliferating RPESCs by added mitogens and expanded in vitro (Blenkinsop et al., 2015; Salero et al., 2012; Stanzel et al., 2014). Passage 2 (P2) RPESC-RPE were differentiated for the indicated times for use in these experiments.

Immunocytochemistry

RPESC-RPE cultured on transwell membranes (Corning Costar) were subject to immunostaining using established methods (Blenkinsop et al., 2015; Salero et al., 2012; Stanzel et al., 2014) with negative controls utilizing secondary antibody alone.

Phagocytosis Assay

POS fragments purified from fresh porcine eyes and labeled with fluorescein isothiocyanate (FITC) (Parinot et al., 2014) were applied to RPESC-RPE lines maintained for 2, 4, or 8 weeks to measure binding and uptake (Figure S2).

Animals and Husbandry

Pigmented RCS rats obtained from Dr. Shaomei Wang and Long Evans rats from Taconic Biosciences, Inc. were maintained under a 12 hr light/dark cycle prior to IACUC-approved procedures.

Subretinal Transplantation

RCS rats at P28–P32 days were provided with cyclosporine (210 mg/L). Under isoflurane anesthesia, a 33-gauge needle was used to inject 1.5 μL of RPESC-RPE cell suspension or BSS vehicle control under the retina; surgical success was confirmed by visualization of a subretinal bleb using optical coherence tomography.

Assessment of Vision

Thresholds for OKT were measured using the computer-based OptoMotry device (CerebralMechanics). Vision measurements were performed by observers masked to the treatment group.

Ocular Histology

Eyes were oriented horizontally along the transplantation site-optic nerve head axis for cryostat (10 μm) or paraffin (5 μm) sections and stained with H&E or with the nuclear marker DAPI. Photoreceptor ONL quantification was accomplished by counting columns of photoreceptor nuclei across the retinal length at 100–150 μm intervals from six adjacent positions, as described (Davis et al., 2016).

SUPPLEMENTAL INFORMATION

Supplemental Information includes Supplemental Experimental Procedures and four figures and can be found with this article online at http://dx.doi.org/10.1016/j.stemcr.2017.05.016.

AUTHOR CONTRIBUTIONS

R.J.D., C.Z., J.H.S., and S.T. led the staged RPESC-derived RPE transplantation experiments. N.A. and G.T.P. oversaw and carried out all vision measurements. C.M., F.M., and S.C.F. oversaw and carried out the phagocytosis experiments. M.N., M.F., T.B., J.S.S., J.H.S., and S.T. developed RPESC manufacture protcols. C.M., T.B., F.M., S.B., C.C., P.L., V.A., P.L.L., and M.N. produced and maintained the RPESC-derived RPE progeny for this work. N.B., S.T., and J.H.S. formulated the statistical plan for data analysis of the visual results while C.M., F.M., and S.C.F. formulated the analyses of the phagocytosis results. S.T., S.C.F., G.P., and J.S.S. oversaw all experiments, data collection, and analysis. J.H.S. and S.T. originally conceived measuring the stage dependence of RPESC-RPE transplantation.

ACKNOWLEDGMENTS

We thank Drs. Shaomei Wang and Bin Lu for the RCS rats and help in establishing subretinal transplant surgery, and Dr. Matthew LaVail for advice on phenotypic analysis of the RCS rat. This work was funded by the Empire State Stem Cell Fund through New York State Department of Health contract no. C028504. Opinions expressed here are solely those of the authors and do not necessarily reflect those of the Empire State Stem Cell Board, the New York State Department of Health, or the State of New York. Drs. Temple and Stern are shareholder in Athghin Biotechnology, Inc. Dr. Glen Prusky is a shareholder in Cerebral Mechanics, Inc.

Received: November 28, 2016
Revised: May 15, 2017
Accepted: May 15, 2017
Published: June 15, 2017

REFERENCES

Alam, N.M., Altimus, C.M., Douglas, R.M., Hattar, S., and Prusky, G.T. (2014). Photoreceptor regulation of spatial visual behavior. Invest. Ophthalmol. Vis. Sci. *56*, 1842–1849.

Algvere, P.V., Berglin, L., Gouras, P., Sheng, Y., and Kopp, E.D. (1997). Transplantation of RPE in age-related macular degeneration: observations in disciform lesions and dry RPE atrophy. Graefes Arch. Clin. Exp. Ophthalmol. *235*, 149–158.

Binder, S., Stanzel, B.V., Krebs, I., and Glittenberg, C. (2007). Transplantation of the RPE in AMD. Prog. Retin. Eye Res. *26*, 516–554.

Blenkinsop, T.A., Salero, E., Stern, J.H., and Temple, S. (2013). The culture and maintenance of functional retinal pigment epithelial monolayers from adult human eye. Methods Mol. Biol. *945*, 45–65.

Blenkinsop, T.A., Saini, J.S., Maminishkis, A., Bharti, K., Wan, Q., Banzon, T., Lotfi, M., Davis, J., Singh, D., Rizzolo, L.J., et al. (2015). Human adult retinal pigment epithelial stem cell-derived RPE monolayers exhibit key physiological characteristics of native tissue. Invest. Ophthalmol. Vis. Sci. *56*, 7085–7099.

Bourne, M.C., and Gruneberg, H. (1939). Degeneration of the retina and cataract, a new recessive gene in the rat. J. Hered. *30*, 130–136.

Brundin, P., Nilsson, O.G., Strecker, R.E., Lindvall, O., Astedt, B., and Bjorklund, A. (1986). Behavioural effects of human fetal dopamine neurons grafted in a rat model of Parkinson's disease. Exp. Brain Res. *65*, 235–240.

Buchholz, D.E., Hikita, S.T., Rowland, T.J., Friedrich, A.M., Hinman, C.R., Johnson, L.V., and Clegg, D.O. (2009). Derivation of functional retinal pigmented epithelium from induced pluripotent stem cells. Stem Cells *27*, 2427–2434.

Conboy, I.M., Conboy, M.J., and Rebo, J. (2015). Systemic problems: a perspective on stem cell aging and rejuvenation. Aging (Albany NY) *7*, 754–765.

Davis, R.J., Blenkinsop, T.A., Campbell, M., Borden, S.M., Charniga, C.J., Lederman, P.L., Frye, A.M., Aguilar, V., Zhao, C., Naimark, M., et al. (2016). Human RPE stem cell-derived RPE preserves photoreceptors in the Royal College of Surgeons rat: method for quantifying the area of photoreceptor sparing. J. Ocul. Pharmacol. Ther. *32*, 304–309.

Diniz, B., Thomas, P., Thomas, B., Ribeiro, R., Hu, Y., Brant, R., Ahuja, A., Zhu, D., Liu, L., Koss, M., et al. (2013). Subretinal implantation of retinal pigment epithelial cells derived from human embryonic stem cells: improved survival when implanted as a monolayer. Invest. Ophthalmol. Vis. Sci. *54*, 5087–5096.

Ganat, Y.M., Calder, E.L., Kriks, S., Nelander, J., Tu, E.Y., Jia, F., Battista, D., Harrison, N., Parmar, M., Tomishima, M.J., et al. (2012). Identification of embryonic stem cell-derived midbrain dopaminergic neurons for engraftment. J. Clin. Invest. *122*, 2928–2939.

Gass, J.D. (1997). Stereoscopic Atlas of Macular Disease, *Vol 4* (Mosby).

Kanemura, H., Go, M.J., Shikamura, M., Nishishita, N., Sakai, N., Kamao, H., Mandai, M., Morinaga, C., Takahashi, M., and Kawamata, S. (2014). Tumorigenicity studies of induced pluripotent stem cell (iPSC)-derived retinal pigment epithelium (RPE) for the treatment of age-related macular degeneration. PLoS One *9*, e85336.

Klimanskaya, I., Hipp, J., Rezai, K.A., West, M., Atala, A., and Lanza, R. (2004). Derivation and comparative assessment of retinal pigment epithelium from human embryonic stem cells using transcriptomics. Cloning Stem Cells *6*, 217–245.

LaVail, M.M. (2001). Legacy of the RCS rat: impact of a seminal study on retinal cell biology and retinal degenerative diseases. Prog. Brain Res. *131*, 617–627.

LaVail, M.M., Sidman, R.L., and Gerhardt, C.O. (1975). Congenic strains of RCS rats with inherited retinal dystrophy. J. Hered. *66*, 242–244.

MacLaren, R.E., Pearson, R.A., MacNeil, A., Douglas, R.H., Salt, T.E., Akimoto, M., Swaroop, A., Sowden, J.C., and Ali, R.R. (2006). Retinal repair by transplantation of photoreceptor precursors. Nature *444*, 203–207.

Mao, Y., and Finnemann, S.C. (2013). Analysis of photoreceptor outer segment phagocytosis by RPE cells in culture. Methods Mol. Biol. *935*, 285–295.

McGill, T.J., Douglas, R.M., Lund, R.D., and Prusky, G.T. (2004). Quantification of spatial vision in the Royal College of Surgeons rat. Invest. Ophthalmol. Vis. Sci. *45*, 932–936.

McGill, T.J., Lund, R.D., Douglas, R.M., Wang, S., Lu, B., Silver, B.D., Secretan, M.R., Arthur, J.N., and Prusky, G.T. (2007). Syngeneic Schwann cell transplantation preserves vision in RCS rat without immunosuppression. Invest. Ophthalmol. Vis. Sci. *48*, 1906–1912.

Parinot, C., Rieu, Q., Chatagnon, J., Finnemann, S.C., and Nandrot, E.F. (2014). Large-scale purification of porcine or bovine photoreceptor outer segments for phagocytosis assays on retinal pigment epithelial cells. J. Vis. Exp. http://dx.doi.org/10.3791/52100.

Prusky, G.T., Alam, N.M., Beekman, S., and Douglas, R.M. (2004). Rapid quantification of adult and developing mouse spatial vision using a virtual optomotor system. Invest. Ophthalmol. Vis. Sci. *45*, 4611–4616.

Salero, E., Blenkinsop, T.A., Corneo, B., Harris, A., Rabin, D., Stern, J.H., and Temple, S. (2012). Adult human RPE can be activated into a multipotent stem cell that produces mesenchymal derivatives. Cell Stem Cell *10*, 88–95.

Schwartz, S.D., Hubschman, J.P., Heilwell, G., Franco-Cardenas, V., Pan, C.K., Ostrick, R.M., Mickunas, E., Gay, R., Klimanskaya, I., and Lanza, R. (2012). Embryonic stem cell trials for macular degeneration: a preliminary report. Lancet *379*, 713–720.

Schwartz, S.D., Regillo, C.D., Lam, B.L., Eliott, D., Rosenfeld, P.J., Gregori, N.Z., Hubschman, J.P., Davis, J.L., Heilwell, G., Spirn, M., et al. (2015). Human embryonic stem cell-derived retinal pigment epithelium in patients with age-related macular degeneration and Stargardt's macular dystrophy: follow-up of two open-label phase 1/2 studies. Lancet *385*, 509–516.

Song, W.K., Park, K.M., Kim, H.J., Lee, J.H., Choi, J., Chong, S.Y., Shim, S.H., Del Priore, L.V., and Lanza, R. (2015). Treatment of macular degeneration using embryonic stem cell-derived retinal pigment epithelium: preliminary results in Asian patients. Stem Cell Reports *4*, 860–872.

Stanzel, B.V., Liu, Z., Somboonthanakij, S., Wongsawad, W., Brinken, R., Eter, N., Corneo, B., Holz, F.G., Temple, S., Stern, J.H., et al. (2014). Human RPE stem cells grown into polarized RPE monolayers on a polyester matrix are maintained after grafting into rabbit subretinal space. Stem Cell Reports *2*, 64–77.

van Meurs, J.C., and Van Den Biesen, P.R. (2003). Autologous retinal pigment epithelium and choroid translocation in patients with exudative age-related macular degeneration: short-term follow-up. Am. J. Ophthalmol. *136*, 688–695.

Warrington, A.E., Barbarese, E., and Pfeiffer, S.E. (1993). Differential myelinogenic capacity of specific developmental stages of the oligodendrocyte lineage upon transplantation into hypomyelinating hosts. J. Neurosci. Res. *34*, 1–13.

Wong, W.L., Su, X., Li, X., Cheung, C.M., Klein, R., Cheng, C.Y., and Wong, T.Y. (2014). Global prevalence of age-related macular degeneration and disease burden projection for 2020 and 2040: a systematic review and meta-analysis. Lancet Glob. Health *2*, e106–e116.